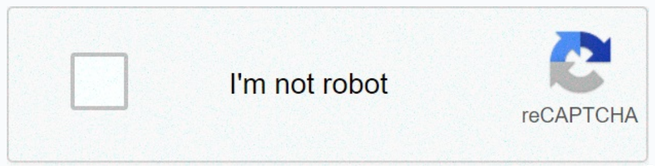

Continue

Dynein and kinesin direction

Chapter 12, pages 511-517, 473-491 In the previous sections we discussed two of the three major types of IUD that make up the cytoskeleton, the intermediate iUD and microtubules. We continue our examination of the cytoskeleton with a look at the role of microtubulation in intracelile transportation and positioning of vehicles and organics. We'll then move on to look at ILAEMENT actin and their functions. How do microtubules function in the intricate transport of vehicles and organics? Microtubules function such as trains in the cell, on which cargo of material such as vehicle or organelle can be transported. In this way, they can guide the movement of material to the cell (note that ILAMAN actin, which we will discuss later, can also function in this way). In addition to moving vehicles and organelle microtubules functions to chromosome movement during cell division, as we've already seen. What causes vesicles and organics to move along these cellular trains? Two families of motor protein, called ash and dyneins, who move onto their microtubul, act like truck towers, attaching to the cargo and pulling it onto the tracks to its destination. There are many types of ash and dyneins, each of which is believed to transport a different cargo. What gives the energy for these protein motor cargoes? Energy for the movement of the motor protein and cargo is provided by ATP, which is broken down into ADP in the process. What is the difference between kinesin and dyneins? Kinesin and dyneins have similarity, but a significant difference is that most noses travel in the further end of the microtubule that are over (i.e., away from the center of the cell), while dyneins travel towards the end less of the microtubule (in the direction for the center of the cell). Thus, kinesin functions carry the broader cargo into the cell, while dyneins function brings cargo to the center of the cell. See Figure 12.51. What are ash and dyneins alike? Although there are detailed differences between noses and dyneins, both engine protein groups have the following features in common: - both have top globilar ATP-required functioning as the engine domain and communicate with the microtubules. - both have a domain that is involved in tying the cargo. See Figure 12.50 How side only goes away from the center of the cell, while dynein are only moved towards it? The headers of the motor protein have stereo-specific stereo, which means that they can be tied to the microtubule only if they are facing the right route. This determines the direction in which they can move. What else does kinesin and dynein do besides freeing their vehicle to their target destination? Kinesin and dinein are involved in maintaining the organics in the correctly positioned cell. Kinesin is thought to be involved in The ER stretches from direction for the peripherality of the cell dyneins thought to be involved in keeping Golgi's complex near the center of the cell. Actin ILAMAN What is actin ILAMAN? ITUNE Actin are the most abundant in three types of cytoskeletal IMBalance. ILAMAN Actin are composed of actin of protein and long shape, thin fiber. These fibers can sometimes be grouped together to make bundles, or crosses to make a three-dimensional network. What are the functions of IAD actin? IVORY Actin are needed for cell movement, phagocytes and cell divisions. They also help in providing forms of the cell They function as trains for entracellular traffic, such as microtubules. They participate in muscle twinge. How is ILAman actin reunited? - Individual actin molecules are protein globulins, each of which can be tied to two additional actin molecules to make a quarter. - These quarters can then make long fibers by the addition of more molecule actin at each end. - Like microtubules, ILAMAN actin has a more delicate and a less delicate end. - The way that shapes actin shapes is very similar to the way that microtubules are assembled (see below). How is the assembly of ILAMAN actin like those of microtubules and how does it differ? Tubulin subunits in microtubules have their GTP bound, and this GTP is hydrolysis of GDP soon after a subunit is added to the growing microtubule. Similarly, monomer actin has the ATP bound to, and this ATP is hydrolysised in ADP soon after the monomer has joined an actin-growing IUD (remember which is who, remembers A for actin and A for ATP). Like microtubules, ILAMAN actin are conveniently disasterd and reasembled. Like microtubules, imature actin can be stabilized by the binding of specific proteins. How does actin ILAMAN affect cell shapes and carry on cell movement? IDIOT Actin is found in large quantities just inside the plasma membrane. The network of actin and protein associated in this region is called the cell cortex and provides a cell form its characteristics. When cells need to move or angular particles, the network actin hides the plasma membrane changes in shape by growth of the IMBalance actin. The change in the IVOry actin leads to the production of proteins in the cell which helps the cell to zoom across a surface or English by fagocytosis. What is myosin? Myosin is an original protein found in muscle, but now it is known to be present in other cells as well. There are various myosin, but myosin-I and myosin-II groups are the most abundant. Myosin muscle belongs to the myosin-II family (see Figure 12.25). What does myosin look like? Muscle myosin (myosin-II) is composed of a pair of identical myosin molecules, and has two blood cellular heads and a baked-coil heart. Clusters of myosin-II molecules tied to each other in form a myosin II. The IAD is organized myosin like a double-headed arrow, with two sets of heads showing away from each other. How to inflate myosin linking to acting IMBAL in muscle cells? The top one on a myosin IADS is associated with an ILAMAN actin series and the other set of headers associated with another ILAMAN actin series (figure 12.23). This arrangement allows sliding of ilaman actin passes to each other and deals. When all bundles of actin and imaging myosin move in this unison way, the bundles can generate a contracted force that is the basis for muscle movement (figures 12.23 and 12.24). Return to Lecture Outlines page. Copyright © 2008 Indira Rajagopal in this study, we are investigating how microtubule engines organize microtubula in Drosophila neurons. We've shown this, during the first steps of axon outgrowth, microtubules show mixed polarity with less-end microtubules pushing the tip of the axon, consistent with kinesin-1 driven out by sliding antipalall microbiles. In later stages, the microtubulating orientation of the axe switches from mixing to uniform polarity and more end-out. Dynein fragile prevents this rearrangement and results in microtubules of mixed orientation of axons and accumulation of microtubule mining at axon tips. Microtubule reorganization requires the recruitment of dynein in the actin cortisol, as actin depolymerization corpus dynein depression, and direct recruitment of dynein in the membrane beyond the actin condition. Our results showed that sliding cortisol dieuz 'minus-end-out' microtubulation from the axon, generating uniform microtubulary array uniforms. We speculate that differences in microtubule orientation between axons and traits might be dictated by differentiating activities of cotal dinein. protein engines can move along the IUD called microtubules to transport proteins and other materials to different parts of the cell. Microtubules are polar ILA, meaning they have two different finishes that have different chemical properties. Protein engines can only move together that IVORY in one direction, for example, the 18 engine proteins generally move in the so-called plus-end direction, while dinein engines move in the opposite direction. A typical nerve cell (or neuron) is composed of a cell body, a long projection called a Ason and many branch-like structures called dendrite. In the axes, microtubules are arranged so that further-ending points are outside, but the microtubules of dendrite are arranged a different way so that many less-finished outdoor points instead. This polarity is crucial for the neuron in deciding which proteins should be transported to axons, and who should go to their dendriters. However, it is not clear how these differ accommodation settled. Here, del Castillo et al. used microscope to study microtubules in the axons of flying fruit neurons. Experiments have shown that in the very early stages of neuron development, the axons have microtubules in mixed polarity. However, by the later steps, the microtubules have become uniform and all the more high-end are headed out. Further experience shows that dinein is responsible for this organization as it pushes micro-end-from the axons. Dynein uses a exhaust made of a protein called Ajin found at the inner surface of the cell and moves the less-end microtubuls into the cell body of the neon. So del Castillo et al.'s find reveals that these dinein engines are responsible for the polarity of microtubules in mature axes. The next challenge is to understand how dynein is attached to the actin scale and why it rearrange microtubules of axons, but not in trait. Neuronal development involves the dramatic morphological reorganization of spherical morphological cells indifferent to highly polarized mature neurons. Developed neurons grow long microtubule based on axle and dendri. Over the past decade, the origins of the mechanical forces that drive process training at neurons have been the subject of numerous studies (Suter and Miller, 2011; Captite and Hoogenraad, 2015). Recently, our lab demonstrates that kinesin-1, a larger microtubling engine, slides microtubules against each other in many types of cells (jolly et al., 2010; Barlan et al., 2013), including neurons, and this sliding plays an important role in neuronal polarization. We showed that microtubulation-sliding microtubule is necessary for initial axon training and reanimation after accident (It et al., 2013b; 2015). This process is most likely for neurodevelopment of many organisms besides Drosophila, as kinesin-driven microtubule sliding involves generating minus-end-august microtubulary models observed in the trait of kaenorhabdis elegance elegance (Yan et al., 2013). The main function is well established in kinesin-1 (also known as conventional side) is the transport of cargo along microtubuls of the cytoplasm. Each kneine-1 molecule is a heterosexual consists of two heavy chains (KHC) and two light ranges (Kuznetsov et al., 1988). Each polypetide KHC has two micro-liquid domains: an ATP-dependent site in the engine domain and a second ATP-independent site in the C-Hackney terminus and stock, 2000; Weger and Rice, 2010; Yan et al., 2013). Kinesin-1 is thought to slide microtubules against one and two such wolf dog domains; one microtubule is used as a track, while the other is transported as a cargo; light ranges not required for sliding (jolly et al., 2010; Yan et al., 2013). Axons have microtubule in uniform orientation and probiotics—end up facing the type axon (Baas et al., 1988; Stone et al., 2008). However, kinesin-1 is a plus-end engine, and therefore can only slide microtubules with the less-finished leading and plus-finished (Figure 1A), which is consistent with the final orientation of microtubules in mature axons. To address this tangible contradiction, we've been asking two questions: First, are microtubules really pushed and the less-ending ones at the initial stages of axon outgrowth, as should they expect if they are pushed by knes-1? Second, if this is the case, how are microtubules with the 'wrong orientation' replaced by microttubules with normal (plus-end-out) orientation in mature axle? To address these questions, we imaged and followed markers of microtubule plus-ending with less-ending of cultivated cleaning Drosophila and Cell S2 at different stages of processing growth. Our findings showed that, in the first steps of neurite training, microtubules were mixing polarity with less-ending being pushed against the plasma membrane; Later, dinein cytoplasmic, attached with the kortex actin, remove less-end microtubules from the cell body, create microtubule array and uniform plus-end orientation. We speculated that the policy of microtubulating dineubule sorting activity could explain the differences in microtubl orientation between axons and traits. (A) Model of microtubule-microtubule sliding drive by kinesin-1. Kinesin-1 slippery antiparallel microtubules apart with less-finished leading (left panel). When kinesin-1 tied to parallel microtubules (right panel), force applied by the two engines of the two microtubules is contrary resulting in no motion net; rather, kinesin-1 cross crossed these microtubules. Large green arrows indicate direction of microtubule sliding; small orange arrows indicate kinesin-1 motion relative to microtubules. (B) A representative cell S2 expresses GFP-CAMSAP3 and mCherry-Turbulent. Note that the CAMSAP3 molecule accumulates in microtubule finish. Two different regions of the cell body (marked 1 and 2) have been magnified in their insets (see Video 2). Low scale, 5 μm. (C and D) Minus-ending of microtubules locates in the tips of growing processes during the first steps of process training in S2 cells. GFP-CAMSAP3 Express Cell S2 is being plated on cover with image 5 min after plate. The plasma membrane was stained with a deep red membrane (red). (C) Last frame in a time-lapse video. Images of different time points in the process are growing in the white box shown in higher magnification. Green arrows indicate position of the most distal CAMSAP3 point; magenta arrows show the tip position in the process (see Video 4). Low scale are 10 μm and 3 μm for main panels and essays, respectively. (D) A graph showing the tip position of the processing and the microtubile displays in the inset of (C) as a two-time function. (E-F) Microtubule plus-end does not collocate with the tip of growing process of S2 cells. (E) Kymographs representative of growing processes from cell express GFP-CAMSAP3 (panel left) or EB1-GFP (right panel). The plasma membrane was attached to a deep red membrane. Note that CAMSAP3 still locates in the tips of the processes during outgrowth event, however EB1 comes by collocating with the tip of the growing processes (low horizontal scale, 10 μm; low vertical scale, 25 s). (F) The graph describing fractions of this time CAMSAP3 or EB1 colocalizes and tips to process them during the growing events. Low error indicates s.d. (CAMSAP3, N = 55 process grows; EB1, N = 51 process grows). Data collected from four independent experiences. <0.0001. (G–I) localization=of=microtubule=minus-ends=at=the=tips=of=the=processes=during=the=initial=stages=bid=neurite=formation=in=cultured=neurons.=(g)=a=still=image=of=4 hr-cultured=neurons=expressing=elav=>PFP-CAMSAP3. The plasma membrane was marked with deep red ink. Note that CAMSAP3 mainly locates in the tips of neurits. Scale bar, 5 μm. (H) Diagram showing the position of the neurite tip and the microtubule-ending minus in the axle showed in (i) as a two-time function. (I am) Still images from a time-laps of a 4 hr-cultured neuron plated as described in (G). Yellow color lines are guided to visualize the growth of neurity. Green arrow indicates the position of CAMSAP3; magenta arrows show position at the tip of the process (see Video 5). Scale bar, 5 μm. We already demonstrated that vessel-1 microtubules slides against each other, and this sliding generates the forces that drive from the initial steps of neurite dependency (Lu et al., 2013b) and axon regeneration (Lu et al., 2015). Because kinesin-1 is a plus-end microtubule engine, it can only slide microbubul with less-end leading and plus-finished finishes (Figure 1A). If this model is correct, it suggests that kinesin-1 must extend neurity by pushing microtubule minus-ending against the plasma membrane during the initial steps of neurit training. Furthermore, because the model predicts that two microtubules have to be in antiparalal orientation to swipe against each other, slippery by xenesin-1 will result in the simultaneous transport of two microtubules in opposite directions (see Figure 1A and the legend for the explanation). Microtubule movement bidires can be thoroughly observed in growing cultural axons Drosophila neuturons using tagged turbulents and a fotokovertin depth (Video 1). Initially testing this hypothesis, we first took advantage of the Drosophila S2 tissue cell culture. Cell S2 provides a good model system to explore the mechanism of process training </0.0001. (G–I)> because they can be induced in the form ofprocess when the integrity of the IOS network is problematic by treatment with either Cytochalasasin D or Latrunculin B (LatB) (Kim et al., 2007; He et al., 2013a). In addition, this system allows us to efficiently study the mechanism of process training by striking down protein candidates with dual-stranded RNA (dsRNA) (Rogers and Rogers, 2008). To study microtubule minus-end distribution of live cells, we ectopically express a fluorescently tagged microtubulary minus-end protein called calmodulin-regular protein spectrin-associated (CAMSAP), also known as Patronin or Nezha. CAMSAP proteins tied to microtubule minus - finished with their stabilizer against depolimerization, making them the perfect candidate of mining microtubule labels - finished (Akhmanova and Hoogenraad, 2015). We initially experienced the GFP-tagged Patronin, the only Drosophila member of the CAMSAP family (Wang et al., 2013), but its expression levels in S2 cells were very low and GFP signals were not ubstly found on microtubules (no data to show). On the other hand, its mammalin autolog CAMSAP3 tagged with GFP express at always higher levels with weighted decorated microtubule finish (Figure 1B). First, we wanted to test whether GFP-CAMSAP3 decorated only one end of microtubules in Drosophila cells. Because the microtubule network is usually too dense to identify both ends of microtubules, we induced the formation of brief microtubuls in cells by partial depolymerization with 25 μMblastine for 1 hr. Tests of these short microtubule fragments demonstrate that only one end of each microtubule contains a GFP-CAMSAP3 plate (Figure 1-figure supplement 1A). In cell S2, spontaneous growth and event shrink associated with the dynamic instability of further-end microtubule were not seen in microtubule finishes decorated by GFP-CAMSAP3, suggest that GFP-CAMSAP3 label microtubule minus-ending in Drosophila cells (Video 2). In addition, EB1-GFP and mCherry-CAMSAP3 never collocate when expressed in the same cell, further confirming less-end localization of CAMSAP3 (Figure 1-Figure Supplement 1B and 1C; Video 3). These findings, along with published data (Tanaka et al., 2012; Hendershott and Vale, 2014; Jiang et al., 2014; Akhmanova and Hoogenraad, 2015), demonstrate that the mammalian GFP-CAMSAP3 seriously marks the microtuble mining-completion of Drosophila. To study localization of mining-finished microtubule in growing processes, we sparked the formation of processing of cell S2 express GFP-CAMSAP3 and began collecting 5 min images after updating cells. At this time point, the nasscent processes were actively growing. We together follow GFP-CAMSAP3 with the plasma membrane using a pit membrane (CellMask Deep Red). We have found that a significant fraction of the growing processes have GFP-CAMSAP3 points to their advice, and that these only lighten when minus-finished microtubule were present in their tips (Figure 1C, D; Video 4). Interestingly, we often observe retraction of the GFP-CAMSAP3 marker from the tip of the process; These events are always considered a pause to outgrowth process (Figure 1C, inset). Quantitative analysis demonstrates that while CAMSAP3 almost always collocates with the advice of the growing processes, the brand plus-finished EB1 could only get through the tips in the processes approximately 30% of the time (Figure 1E, F), suggesting that in this dynamic microtubule step does not play a big role in development processes. To investigate the localization of microtubule minus-end of Drosophila neuron, we have created a transgender fly that expresses GFP-CAMSAP3 under the UAS developer. Neurons were harvested and cultural in the brains of lava express GFP-CAMSAP3 driven by pan-neuronal promoter Helav-Gal4 (Egg et al., 2013; Read et al., 2015) (see Materials and methods). We visualized microtubulating minus—ending in growing neurities in initial growth stages (4 hr after plate), when neuron began developing processes (length = 9.96 μm, s.d.d.± 4.5μm, n = 50 axons). We found that, as in cell S2, the growing neurities have GFP-CAMSAP3 points to their advice in neurities, and localization of the points of advice are precisely correctly correlated with excess neurism (Figure 1G-I; Video 5). Altogether, this data shows that at least a fraction of the growing microtubules neurite has the 'wrong' orientation (min-end-out). Localization of microtubulated minus-end(s) to tip the top correlates and outgrowth neurites, consistent with kinesin-1 push minus-end microtubules against the plasma membrane drive beyond the initials. If kinesin-1 slipped antiparalel microtubules in the first stages of axon training, the growing neurites should initially have microtubules and mixed orientation (Figure 1A and the legend for the explanation). To test this prediction, we imagine and follow the direction of the more-end microtubule marker, EB1-GFP, in the axle of cultured colors of different time points after patches. Quantitative analysis of EB1-GFP comes using software tracking (see Materials and Methods) demonstrates that, shortly after updating, growing neurities have EB1 coming moving in both anterograde direction and retrograde direction (Figure 2A, B; Video 6). The microtubule orientation of asons remains mixed during the 1st day of culture. In 36 hr, the fraction of EB1 retrograde comes starting downturn, and in 48 hr, axons developers have been mostly filled with further-end-august microtubules (Figure 2A, B; Video 6). These results demonstrate that axons initially have microtubule array and mixed orientation. (A and B) Microtubuls Axonal gradually acquired uniform orientation during development. (A) Representative Always Imaging EB1 - GFP Express kiltire pou 4 hr, 21 hr, oswa 48 hr. Kymographs nan EB1 vini yo montre anba a imaj korespondan. Magenta ak flech vet endike direksyon EB1 vini mouvman (plis-fen-an ak plis-fen-soti, respektivman). Liy jon jon defini zon nan nan axon a itilize pou trase EB1-GFP kymographs (gade Videyo 6). Echel ba, 10 μm. (B) Fraksyon nan EB1-GFP vini dirije nan direksyon pwent an nan neurite yo (plis-fen-soti) oswa ko a selil (plis-fen-an). Gade Materyel ak metod pou yon eksplikasyon nan EB1 vini quantification. Ba ere endike s.d. (4 hr, n = 35 axons ak 761 vini; 21 hr, n = 33 axons ak 408 vini; 36 hr, n = 33 axons ak 526 vini; 48 hr, nou = 25 axons ak 299 vini). * p = 0.034, <0.0001, n.s. = not significant.= data= collected= from= three= independent= experiments. (c= and= d)= dynein= knockdown= causes= mixed= orientation= of= microtubules= in= axons.= (c)= representative= still= images= of= control= (elav-gal4)= and= dynein= knockdown= (two= different= dhc= shrnas= driven= by= elav-gal4)= 48 hr-cultured= neurons= expressing= eb1-gfp.= magenta= and= green= arrows= indicate= directions= of= eb1= comet= movement= (plus-end-in= and= plus-end-out,= respectively)= (see= video= 7).= scale= bars,= 10= μm.= (d)= fraction= of= eb1-gfp= comets= directed= toward= the= tip= of= the= neurites= (plus-end-out)= or= the= cell= body= (plus-end-in).= error= bars= indicate= s.d.= (control,= n=28 axons= with= 269= comets;= dhc= rnai#1,= n=45 axons= with= 928= comets;= dhc= rnai#2,= n=30 axons= with= 454= comets).=></0.0001,> <0.0001. data= collected= from= three= independent= experiments. (e)= dynein= knockdown= in= neurons= results= in= accumulation= of= microtubule= minus-ends= at= the= tips= of= neurites.= images= of= 48 hr-cultured= neurons= expressing= elav=>*pFP-CAMSAP3 (panel kite) oswa elav>GFP-CAMSAP3 + DHC RNAi (panel dwa). Panno anba yo se mayifikasyon nan zon yo jon-bwate. Echel ba, 10 μm. (F-G) Dynein inactivation induces antiparallel mikrotubule etalaj nan S2 pwosesis selil yo. (F) imaj reprezantatif nan kontwol (kontwol) oswa DHC dsRNA-trete selil S2 eksprime EB1-GFP. Magenta ak flech vet endike plis-fen-an oswa plis-fen-soti direksyon nan EB1 vini mouvman, respektivman (gade Videyo 8). Echel ba, 10 μm. (G) Graphs dekri direksyon EB1-GFP vini nan pwosesis yo nan selil S2 kontwol, ak selil apre frape DHC, p150Glued, Lis1, oswa NudE. Ba ere endike s.d. (Kontwol, nou = 55 selil ak 1747 vini; DHC RNAi, nou = 50 selil ak 1929 vini; p150 RNAi, nou = 26 selil ak 2282 vini; Lis1

RNAi, nou = 33 selil ki gen 3359 vini; NudE RNAi, nou = 24 selil ki gen 2518 vini). p = 0.001-0.0001, *p <0.0001. Data collected from three independent experiments. (H–I) Dynein inactivation in S2 cells results in accumulation of microtubule minus-ends in the process tips. (H) Representative images of untreated (control) or DHC dsRNA-treated S2 cells expressing GFP-CAMSAP3. In S2 cells, CAMSAP3 particles display a scattered data= collected= from= three= independent= experiments. (h–i)= dynein= inactivation= in= s2= cells= results= in= accumulation= of= microtubule= minus-ends= in= the= process= tips.= (h)= representative= images= of= untreated= (control)= or= dhc= dsrna-treated= s2= cells= expressing= gfp-camsap3.= in= control= s2= cells,= camsap3= particles= display= a= scattered=></0.0001. Data collected from three independent experiments. (H–I) Dynein inactivation in S2 cells results in accumulation of microtubule minus-ends in the process tips. (H) Representative images of untreated (control) or DHC dsRNA-treated S2 cells expressing GFP-CAMSAP3. In control S2 cells, CAMSAP3 particles display a scattered > </0.0001.> </0.0001.> and some less-finished in processing tips. In dinein RNAi cell S2, CAMSAP3 particles robustly accumulate in the tips of their processing. Balance low, 10 μm. (I) Graphs displaying fractions of S2 cells show the phenotypes that are described in (H). (Control, n = 117 cells; DHC RNAi, N = 84 cells; p150Glued = 90 cells; Listing1 RNA1, n = 83 cells; NudE RNAi = cell 79). DHC, dinein heavy chain. pHC RNAi animals developed in the third stage <0.0001. data=collected=from=three=independent=experiments.= our=data=suggest=that=some=sorting=mechanism=is=responsible=for=the=elimination=of=microtubules=with=the='wrong'=(plus-ends=the land=soma)=orientation=from=maturing=a='maturing=xons.=we=hypothesized=that=this=sorting=factor=is=cytoplasmic=dynein=because=it=has=been=reported=that=mutations=in=dynein=light=intermediate=chain=or=dynein-cofactors=(nude)=are =required=for=uniform=microtubule=orientation=in=axons=of=drosophila=dendritic=arborization=(da)=neurons=(zheng=et=al.,=2008;=arthur=et=al.,=2015).=to=character=character theize=role=of=dynein,=see=expressed=too=different=shrnas=targeting=dynein=heavy=chain=(dhc)=using=elav-gal4=to=specifically=knock down=dynein=in=neurons.=elav=>enstar larval; however, the lokootion was severe having problems with most deaths before they reached the pupae stage (data not shown). Furthermore, none of the survival slave >DHC RNAi pupae eclosed in adults. We cultured neurons found in the brain of the third helave installation >DHC RNAi lavae. Our laboratory has already shown that mitochondrial movement has substantially decreased in helav >DHC RNAi RNAi, indicating that the activity of dynein containing problems of these neurons (Lu et al., 2015). Following the microtubule orientation after dinein depression, we genetically combine transgens coding DHC RNAi with EB1-GFP or GFP-CAMSAP3. We first ntify the direction of the EB1 coming in neuron grown for 48 hr; At this time point, microtubules in the axes of control urons are mostly oriented and more-end-out (Figure 2B). Analysis of EB1 comes in Helav>DHC RNAi 48 hr-neurons reveal that axons including microtubule array of mixed orientation (Figure 2C, D; Video 7), suggests that dinein needed to remove less-end-august microtubules from axons. Interestingly, while microtubule minus-finishing of control neons, as visualized by GFP-CAMSAP3, have spread throughout the length of the axons, the inactivation of dynein resulting in dramatic accumulation of the mining-end markers of neurite tips (Figure 2E; controls, panels left; DHC-RNAi, rights panel). To further investigate the role of dinein in organizing microtubular array of cell processing, we again examine the Drosophila S2 cells. Cell treatment S2 and dsRNA dsRNA efficiently hit DHC (Figure 2-Figure 1A, B). Recapture the neronal phenotype, dynein depression in S2 cells resulting in process and vini </0.0001.> </0.0001.> in both directions (Figure 2F, G; Video 8). We also examine the GFP-CAMSAP3 distribution of S2 processes. In control cells, GFP-CAMSAP3 has a large, scatter point distribution (Figure 2H, left panel). Dynein depression produces a striking highlighting mass accumulation of CAMSAP3 in the tips of processing (Figure 2H, I). Overexposed images of these processes reveal that less-ending could still be found in other areas of the processes (Figure 2-Figure Supplement 2). Identical phenotypes (mixing the polarity of GFP-EB1 come with the accumulation of CAMSAP3 in these tips in their process) have been observed after striking down several diney cofactors (p150Glued, Lis1 or NudE; Figure 2G–I; Figure 2- Figure supplement 1B for striking efficiency). Highlighting the minus-end microtubule advice advice and S2 processing of cell RNAi dinein is consistent with the idea while kinesin-driven sliding remains intact, the sorting mechanism is inactivated by delenere. In many organisms, the organization and orientation of the mitotic spindle requires attachments of sittoplasmic dynein in the cell cortisol (Laan et al., 2012; Kiyomitsu and Cheeseman, 2013). We hypothesis that organizations of microtubules in axons, such as the organizations of the mitotic spindle, require anchoring of dynein in the cortical network of IUD actin. To test this idea, we depolymed the IUD actin into cultivated Drosophila neuron by treatment with LatB and microtubulary microtubulation orientation in axle. We found that increased concentrations in LatB gradually reduced the amount of F-actin, as deemed by the intensity of rhodamine-phalloidin spots (data not shown). In parallel with F-actin depolymerization, axons displayed a increased fraction of microtubules and plus-finished faces in the cell body (Figure 3A). At a high concentration of LatB (10 μM), when practically no F-actin can be detected, over half of all EB1 comes moved towards the cell body, demonstrating that depolymerization of actin induced random microtubule orientation at neurons (Figure 3A). Treatments with high laboratory concentrations also induced the minus microtubulary accumulation of the tips of the axons of helav >GFP-CAMSAP3 neuron (Figure 3B). (A) Actin depolymerization of cultural neuron results in formation of axons and antiparale microtubules. Graphs describing fractions of Axonal EB1 come moving in every direction in 48 hr-cultured neuron treats with different concentrations in LatB. Low error indicates s.d. (0 μm Latb, n= 34 axons and 905 come; 1 μM LatB, n = 20 axons and 852 come; 2 μM LatB, n = 37 axons and 102 come; 10 μM Labt, n = 15 axons and 547 come). *p = 0.0144, *p<0.0001. data=collected=from=three=independent=experiments. (b)=latb=treatment=induces=accumulation=of=minus-ends=in=neurite=tips.=a=48 hr-cultured=neuron=expressing=elav=>GFP-CAMSAP3. Panel on </0.0001.> the rightareas of the previous neurite tip or 14 hr after LatB washout. The overexposed images show the description of the neurite. Note that LatB movement indicates the retrograde movement of CAMSAP3 decorated microtubules. Low scale are 10 μm and 5 μm, respectively. (C–E) Actin depolymerization of cell S2 results in the formation of process and antiparale microtubule orientation with an accumulation of microtubule mining-completion of the tips of processing (compared to Figure 2F-H). (C) Graphs that describe the direction of EB1-GFP come through S2 processing. Low error indicates s.d. (Control, n = 20 cells and 1833 come; 10 μM LatB, n = 22 cells and 2408 come). p<0.0001. Data collected from three independent experiences. (D) Graph describing the distribution of GFP-CAMSAP3 to the processes of S2 cells treated with 0.5 μM (control) or 10 μM Latb (Control, n = 82 cells; 10 μM Labt, n = 75 cells). p<0.0001. Data collected from three independent experiences. (E) confocal image of a cell S2 express GFP-CAMSAP3 plated to 10 μM Latb. Note that GFP-CAMSAP3 accumulates in process guidance. Bar scale, 10 μm. (F and G) Recruitment of dynein into actin cortical toggle the sorting activity at dinein. (F) Representative always images from time-laps of cell S2 Express GFP-CAMSAP3 plated for 4 hr in attendance at 10 μM in Labot. In control cells, microtubulate minus-finish staying in the tips of their processing (left panel). LatB bus causes a cleaning of microtubul minus - ending out of process (panel precedent). Dinein knockdown containing the microtubular sorting problem after LatB was kicked with minus-end microtubule remains clusters of tips (see Video 9). Bar scale, 10 μm. (G) Schematic representation of the mud lab artifacts (microtubule minus-end are represented in magenta). In latB presence, dinein is uncovered in the plasma membrane, preventing its sorting activities (top panel). After was choice, dynein recruited into the plasma membrane by corrtic acctinents, causing robust microtubule sorting and transport of less-end-august microtubules towards the cell body (bottom panel). (H–I) Direct recruitment of dynein to the membrane bypass the F-actin condition for sorting microtubiles. Endojene dynein can be recruited into the plasma membrane of S2 cells coexpressing FRB-GFP-BicD and GAP43-FKBP. In the presence of 10 μM LatB, cortical actin is depolymerized and therefore dinein remains solid in the sittoplasm. In addition to 1 μM rapalog induce the recruitment direct to the dinein-BicD complex of the plasma membrane (see Materials and methods). The sorting activity at dinein was followed by Imagine mCherry-CAMSAP3. (H) Always images from time-laps to a previous S2 cell (panel left) and after addition to rapalog (middle and right panels). Magenta and green arrows represent the position of the membrane and the CAMSAP3, respectively. Note that CAMSAP3 signals move towards the cell body when rapalog is added while there is not a substantial retraction in their process (see Video 10). If the same experience is conducted in RNAi DHC cells, the addition of rapalogs does not feature retrograde transport of the min-end microtubuls from the tips to process (see Video 10). Bar scale, 10 μm. (I) Schematic representation of the recruitment of BicD-dynein (microtubule mining - end are represented in magenta). In the presence of LatB, dinein is solid in the cytoplasm. In addition to directly recording rapalogs of the membrane in the presence of BicD recruitment protein, activate dinein activity in and retrograde transport of microtubules into the cell body. (J) Fraction of processing that appears retrograde movement of less-end microtubules as CAMSAP3 signals. (Control, n = 122 processing; DHC RNAi, N = 99 process). DHC, dinein heavy chain. following data shows that actin depolymerization of phenocopied depression dynein in axons, suggesting that sort dinein cortical stupidity microtubules. If this hypothesis is correct, LatB autout should restore the recruitment dynein to the kortex, and the microtubular sorting activity of dinein cotal should remove the minus-end-from the tip of the axon. To test this prediction, we wash out LatB and follow the localization of GFP-CAMSAP3. We observe that the lab indicates the removal of GFP-CAMSAP3 from axon tips without affecting the length of the axon (Figure 3B). It should be mentioned that LatB orthopedic was not resulting in the normal dispersion of less-ended sets the length of the axon observed in neuron controls (Figure 2E, panels left). Instead, they remained clustered in the shabby, most likely because by the time of drugs were fucked these mining microtubules had already crossed into a package. To observe the sorting activity of cotal dinein in real time, we again use S2 cells. As in the case of neurons, the treatment of S2 cells with high concentrations of laboratories produces training in processes with microtubules of mixed polypharity (Figure 3C) and massive accumulation of less-ending of the tips (Figure 3D-F; Video 9). Strikingly, LatB bus has caused robust movement of GFP-CAMSAP3 which marks minus-completion from the tips of processing towards the cell body (Figure 3F, middle panel; Figure 3G; Video 9). However, if the same experiment was conducted after dynein hit, retrograde transport of minus-end microtubule was not observed and the min-finished caps remained in the guidance of process (Figure 3F, rights panel; Video 9), directly demonstrating the role of cortical dynein is removed from less-end-august microtubules from processing in the cell body. To further confirm that dynein and actin ILAMAN are inserted into the same microtubule-sorting route, we have decided requirement for imaging actin does not directly recruit dynein into the cell membrane. For these experiments, we used a dinein recruitment tool developed by the Akhmanova and Hoogenraad Laboratories (Hoogenraad et al., 2003; Capt. et al., 2010), containing the activator Dinein Bicaudal D (BicD) stuck in an FRB domain (FRB-GFP-BicD). The FRB-BicD-dynein complex then be recruited to any region of interest by coexpression of a protein targeting the tangled protein in a FKBP domain. This FKBP domain is chemically dimerized with the FRB domain in the presence of rapalogs (a cell-permeable analog molecule of rapamycin) (Clackson et al., 1998). To confirm that the FRB-FKBP dinein dinein recruitment system works in Cell Drosophila S2, we first coexpressed a GFP constructor fused FRB (FRB-GFP) and the peroxisome membrane-targeted peptide signal coupled in fluorescent protein red (PEX3-RFP-RFP-FKBP). In the absence of rapalog, the GFP signal appears soluble in the cytoplasm. In addition to rapalog recruit frb-GFP for peroxisomes (Figure 3-figure supplement 1A). We next use this system to directly recruit into the plasma membrane. For targeted membranes, we pasted the transmebrant domain of GAP-43 (Heim and Garibeck, 2004) and FKBP and coexpressed this construction with the FRB-GFP-BicD in cell S2. To visualize the recruitment of BicD in the membrane of these cells, we use total internal reflection fluorescence (TIRF) microscopy to signal the GFP image before and after the addition of rapalog. Quantification showed that the addition of rapalog significantly increased the intensity of fluorescence to GFP due to the recruitment of BicD citoplasmic in the plasma membrane (Figure 3-figure supplement 1B). We next tested whether direct recruitment of dynein in the membrane using rapalog could drive microtubule sorting in the absence of cortical actin. To test this hypothesis, mCherry-CAMSAP3 was used to track the localization of the minus-finished microtubule. In the absence of rapalog, CAMSAP3 accumulates in the processes of S2 cells treated with 10 μM LatB. Time-laps imagined before addition to the drug reveal that these CAMSAP3 clusters, which mark the less-end position, were either static or pushed against the plasma membrane (Video 10). However, when the complex BicD-dynein was recruited to the membrane by addition to rapalog, CAMSAP3 marked microtubule mining-ends crossed away the tip, towards the cell body (Figure 3H, panel top; Figure 3I; Video 10). The same association made of knockdown DHC cells did not show removing this from min-finished microttubule (Figure 3H, bottom panel; Video 10). Taken together, this data confirms that dinein is responsible for microtutubulary sorting, and this activity requires the attachment of the engine to the kortex ombudsman by IUD actin. Mature axons have microtubule array of uniform polarity and plus-ends away from the cell body (plus-end-out). Here, we follow both plus-finished and less-finished completion of microtubul to the axes of Drosophila's culture netrons in different stages of development. Our data also showed that the axonal microtubule network underwent dramatic reorganization during development. In the first stage of neurite training, minus-in microtubules sliding are pushed against the plasma membrane, generating the forces that drive first beyond neugraphy. In this scene, growing neurites have microtubulary array of mixed orientation. However, later in development, axonal microtubulating arrays are reoganized from the uniform mix (plus-end-out) orientation, consistent with well established microtubule organization described in mammali (Baas et al., 1988) and Drosophila axons (Stone et al., 2008). Here, we demonstrate that cortical dynein driving this transition by sliding with less-end expertise — from microtubules to axis to the direction of the cell body. We have already demonstrated that initial neurite training in Drosophila neuron requires microtubule-microtubule sliding driven by kinesin-1. Knockdown of kinesin-1 in main neurons issues the motulity of microtubul interface and causes neuron fail to develop axons (Lu et al., 2013b). This was surprising because the nose-1 is a micro-end plus-end engine and thus can only slide microtubules with less-end leading and high-end finishes. In addition, the consideration of symmetry dictates that sides slippery antiparale antiparale against each other; if microtubules are oriented parallel to one another which might pack rather than slippery ones (Figure 1A). Both of these considerations appear to contradict established literature on microtubule polarity in axons. In this work, we have experienced two more experiences supporting the idea that side by sliding sliding-1 activity leads the first steps in training neurité (Read et al., 2013b). First, the neurit growing nascent has microtubular array and mixed polarity. As mentioned above, this antiparalal orientation is required for microtural sliding by cnesin-1 (Figure 1A). Second, the less-ended microtubule is pushed against the plasma membrane of the tips to process, generating the strength for neurit growth. Latest experimental data reveals that 'mitotic' kinesin, such as kinesin-5 (Nadar et al., 2008; Nadar et al., 2012) and Kinesin-6 (Lin et al., 2012; del Castillo et al., 2015), play a significant role in the settlement of axon outgrowth. The well-established function of these mitotic engines is to reorganize and stabilize the spindle of mitotics facilitating chromosome segregation. These engines accumulate in the midzone spindle where antiparale microtubul comes from opposite overlapped poles. Our work shows that developing Drosophila axons, such as the spindle midzon, are filled with antiparale microtubl array. That configuration suggests that the same mechanisms control the mitotic spindle could be used to control axonal outgrowth (Baas, 1999). Interestingly, 'mitotic kinesins' control neurites exceed both in mammalian and Drosophila systems, which support the idea that the molecular players who drive axon initiation and outgrowth of Drosophila can be maintained across species. Our data show that microtubules mining -end-out are still observed in the early stages of neuris training, while in later the later stages the majority of microtubules of axons have further-ended them out, as reported in multiple publishing papers (Baas et al., 1988; Stepanova et al., 2003; Stone et al., 2008). Therefore, neurons must activate an additional sorting mechanism that eliminates these 'mal' polarity microbula from axons. Previous studies report that protein dynein and dinein-associated are required for correct microtubule orientation incorrect axons of Drosophila sensor neurons (Zheng et al., 2008; Arthur et al., 2015). Our findings are using cultural neurons in full accordance with such science, as dynein cknodown caused mixing blended polarity into axons. Interestingly, several sciences have linked dinein-mediated microtubule reorganization acts, both in interphase (Mazel et al., 2014) and in mutoss (Kotak et al., 2012; Kiyomitsu and Cheeseman, 2013). In this study, we have shown that depolymerization of IMMERsion actin (including cortical actin) using high concentrations of LatB causes the same damage to microtubule orientation as dynein knockdown. Recovery of cortical actin after result was the effective drug choice for effective removal of less-end microtubules from the tips of processing. In addition, the requirement for actin can be efficiently bypassed by direct recruitment of the dinein machine directly from the plasma membrane. Therefore, we propose that sorting microtubule depends on the activity of cytoplasmic dining attached to the meshwork of corrtic iMA. However, as we didn't get full recovery of the wood type distribution of microtubules in our LatB lab or dynein-membrane recruitment experience, it is likely that additional proteins that link actin with microtubulous routes to the neuron are involved in microtubulous organizations; a good candidate is well characterized actin-microtubule crossing short protein stops (Lee and Kolodziej, 2002). In addition to sorting the activities described in this work, other groups observed that dinein activity is required for upscale axon (Ahmad and Baas, 1995; Ahmad et al., 1998; Grabham et al., 2007). A recent study by Miller et al. reported that dynein generates strength that pushes the advanced cytoskeletal meshwork during the axonal upscale of cultural detectors chic (Roossien et al., 2014). In accordance with the data, we predict that the corrical can promote axon outgrowth after the first steps to outgrowth neurit, when microtubules are sorted into a more end-out orientation. Because the direction of dynein-powered forces dictated by the intrinseic orientation of microtubules, microtubules and less-out are reinsented towards the cell body, when we consider the further-end microbes transported to the tip of the axon. Therefore, dinein-driven microtubule transport can not only remove microtubules with the wrong orientation (min-end-out) but also push microtubules into the right orientation (plus-end-out) towards tip axon. Besides the dynein role of developing neurons, dynein can play an important role in axonal microtubule maintenance. Microtubule polymers, like other protein structures, require turning the subunit to maintain their integrity. He proposed that several severe protein lots are able to fragment microtubules in short pieces (McNally and Vale, 1993). In this scenario, short microtubule grains are generated that can be redirected by streaming force in either direction (plus-end-in or more-end-out) and equal probability. Indeed, active bidirectional transportation of microtubulary fragments short of the axons was described in cultural hippocampal neurons (Liu et al., 2010). The authors proposed that the transport of these microtubule fragments be shortened driven by dynein. Our prediction is that microtubulary fragments transported in the retrograde direction should be oriented and further-ended towards the cell body while enthusiastically trans fragments should have the opposite orientation. It has been shown in many different model systems that nose-1 and dynein are the two major engines involved in reorganized cytoplasmic microtubules (Fink and Steinberg, 2006; Traube et al., 2006; Jolly et al., 2010; Mazel et al., 2014). Both engines play an important role in axon training. However, the contribution of each engine is likely different in different developer stages (see patterns described in Figure 4). In the spheres that conform indifferent cells, kinesin-1 engines glide antiparal microtubules perpendicules to the plasma membrane and the less-end-leading (Figure 4A). This sliding generates the strength that breaks the symmetry of the cell and indicates a deformity of the plasma membrane to start the growth of neurites. During this stage, the role of dinein cotal is probably limited by sterical restrictions. Dinein cortical can only slide tangential microtubules into the plasma membrane, and therefore dineu-mediated movements cannot distort the membrane and initiate outgrowth. In the next step, nascent neurites have antiparale microdulable array (Figure 4B). This configuration allows Ash-1 to continue to drive antiparale microbule sliding. Once the processes begin to form, the new geometry will allow dynein cortical contributors both microtubule organizations with outgrowth neurites. Cortical dynein in the neurit cortex can only slide microbubules parallel to the axle of the process. This contribution to cortical dinein increases as the processes grow longer (engaging more dineu molecules) and thinner (allowing dynein to reach a larger fraction of microtubules in their processes). (A) Kinesin-1 induced sliding through antiparale microturals initiated the process formation. Note that in this dynein cortical stage can only slide parallel microtubules with the plasma membrane, suggest that dynein is not involved in the initiation of processing. (B) Short neurites include antiparallel microtubulating array. Under this configuration, kinesin-1 always slippery microtubules and minus- finish them out, and cortical dinein can start removing minus-end-out microtubules in the cell body. (C) Due to continuous sorting-powered sorting activities, the growing axon is mostly filled with uniformly oriented more-end-out microtubules. At this stage, dinein can continue removing minus-end-out microtubules, and can contribute to axon elongation by pushing further-end-outtubules towards the tip (see Roossien et al., 2014). Note that at this stage, kinesin-1 engines only pack parallel microtubules and do not contribute to microtubl sliding or outgrowth. The triangles on the right represent the engine contributions at each stage. There are two possible microtubule orientations in the neurite that can interact with cytoplasmic dynein. Microtubules with end-out minus (microtubule in the 'trunk' polarity) will be moved by dynein towards the cell body, therefore eliminating them from processing them. At the same time, dinein can interact with and push more-end-out microtubules to move them towards axon advice, and thus contribute to the forces that drive axonal growth (Figure 4B). As a result of this continuous sorting activity in dynein, developed axons include uniform microtubule array and distal plus-end ones (Figure 4C). Under this new microtubule configuration, kinesin-1 contributes little to microtubl sliding (as the microtubl antiparael array is needed for cooking engaged in sliding), but instead favors its bundling activity (Figure 1A, right panel). In addition to its contribution to neurite growth, coriander dinein can have a significant role in axon maintenance, removing nascent microtubules of evil orientation that can appear in the axon either due to new microtubule polymerization or due to the server of pre-existing microtubules. Because axons and dendrite are common morphological characteristics observed in urons from moody ancestors to mamal, we postulate that the same molecular mechanism introduced here for axon training in Drosophila is maintained in other organisms. Of course, this 'microtubule-centric' Do not describe all the mechanisms involved in axon training, and clearly leave out the critical question of axon advice, but it provides key roles for multiple microtubule engines involved in axon training and microtubule organizations. Microtubule orientation differs between axons and traits. While axons are filled with uniform microtubules and more-end-out, dendrite has either microtubules of mixed orientation (mamilian neuron) (Baas et al., 1988) or a majority of microtubul min-end-out (Drosophila and C. neon elegance) (Stone et al., 2008; Yan et al., 2013). We speculate that neurons selectively employ the corrtic dynein to dictate which of the nascent neurites will become axon in the future. It is likely that the microtubl sliding activity or efficiency of recruiting dinein can come down to dendriters. This hypothesis is in accordance with a recent study of Drosophila da neurons sensory which shows that the inconvenience of NudE, a dinein koktor, issues microtubule orientation in axle, without affecting the orientation of dendritic microtubules (Arthur et al., 2015). In addition, Yan et al. directly demonstrates that container-1 (unc-116) is required for less-end-out orientation of microtubules in described (Yan et al., 2013). These observations support the idea that the activity of cortical dynein downregulated to dendrite, thereby preserving the first minus-end orientation of microtubules created by nose. Future experiences are required to unlock how dynein reacts with cortical actin and how microtubulating-sorting controls through neons. Request a detailed protocol to visualize microtubule minus-finishing of the Drosophila S2 cell system, a CAMSAP3 mouse encoding cDNA (Jiang et al., 2014) has been closed to the pMT-GFP and pMT-mcher back by Noti-Agei energies site restrictions to generate GFP-CAMSAP3 and mcher-CAMSAP3. GFP-CAMSAP3 was also close to UASpp backbone by KpnI-XbaI to create a flying drosophila transformation containing the UASP-GFP-CAMSAP3 by standard P component-mediated transformation. A plasmid encoding EB1-GFP under endojene developer (pMT-EB1:EB1-GFP) was used to visualize microtubule plus-ends in cell S2. For recruiting experience, all constructions have been closed to pAC.V2014, a modified version of pAC5.1 that has multiple cloning sites (KpnI-NheI-BmtI-HindII-AscI-AscI-Noti-Noti-XbaII-EcoRV-XhoI). FRB-GFP and PEX3-mRFP-fragments FKBP from pβActin-GFP-FRB and pβactin-PEX3-mRFP-FKBP plasmids (Capts et al., 2010) Being subcloned in HindIII-Noti and HindIII-EcoRI sites to generate pAC.V2014-FRB-GFP and pAC.V2014-PEX3-mRFP-FKBP. Drosophila BicD CDNA (LD17129 from DGRC) has been lightened by PCR and lightest of these Asci-Noti sites in pAC.V2014-FRB-GFP to create pAC.V2014-FRB-GFP-BicD. FKBP fragments were inserted into pAC.V2014 using the following AscI-EcoRI sites for pAC.2014-FKBP. To recruit the FKBP domain of the membrane, sequence DNS coding domains transmebrant GAP-43 (MLCCMRKQQVEKEDKI) was lighted in the following Kpni-Asci sites in pAC2014-FKBP to create pAC2014-GAP43-FKBP. Request a detailed protocol on stolen stocks and oceans being cultivated on standard food correlated based on Bloomington Stock Center recipes at room temperature. Stock of the following stolen lines used in this study: UASp-tdEOS2-αtub84B (2nd and 3rd insertion chromosomes) (Lu et al., 2013b), ubi-EB1-GFP (3rd insertion chromosomes) (Shimada et al., 2006); UASt-EB1-GFP (3rd insertion kromosome) (Roller et al., 2007); elav-Gal4 (3rd chromosome election, Bloomington Stock #8760) (Luo et al., 1994); UASp-GFP-CAMSAP3 (2nd election chroform, created in this study); DHC64C-RNAi TriP line, (Valium 20, stock Bloomington #36698, 3rd attP2 election, targeting DHC64C CDS 1302–1322; Valium 22, Bloomington Stock #36583, 2nd chromosome attP40 election, targeted DHC64C CDS 10044–10064). Shares of yw; DHC64C - TRiP RNAi - Valium22; ubi-EB1-GFP, yw; UAST - EB1 - GFP; DHC64C - Triple RNAi - Valium20, and yw; UASp - GFP - CAMSAP3; DHC64C-TriP RNAi-Valium20 was produced using standard balancing procedure, with oceans and helav-Gal4 to examine EB1-GFP or GFP-CAMSAP3 in the DHC64C knockdown. Requesting a detailed neuron's main protocol was found in the brain of the 3rd Lava enstar as previously described (Lu et al., 2015). Neurons were coated on concanavalin A-coated clips in Schneider's extra medium (20% serum bovin fetal, 5 ml insulin, 100 μg/ml penicillin, 100 ml streptomycin, and 10 μg/ml tetracycline). To purchase borderly depolymerization, neurons were plated in Xpress medium for 2 hr before being addition to LatB. Drosophila S2 cells have been cultured as previously described (Barlan et al., 2013). To provoke the formation of processing of S2 culture, the cells were plated in the presence of 0.5μM LatB. For essex disorder in S2 cells, cultures of 1.5 x 106 cells/mL were treated twice and 20 μg of dsRNA (1 day and 3 days) and cell analysis was performed within 5 days. Double-stranded RNA was transcribed in vitro and T7 polymeras, and purified using extraction liquids. The first ones used to create T7 models from stolen young manomic DNS were as follows. T7 developer sequences (TAATACGACTACTACTAGGG) are added at the end of 5′ at the end of each primary). DHC, Advanced, AAACTACAGAATTAACCCC; reverse, TTGGTATGTCACT(jolly et al., 2010); p150Glued, advanced GAGTGATGAGATGAGATGACCC, reverse GTTGCGATGTGTCGTTCCAGTTC; List1, advanced GGTGATATTACGGATGATGATCAGTACTGTGA, reverse GGAGGTCAGGAGAGGATGGCGGTAGTAGTAG; NudE, Forward, GCTCAAGTGATGGATGCATGCGCGATTC, Reverse, CTCTCTCATCTTAGTAGTAGTTCGTCGTCGCGC. To provoke the formation of microtubule fragments, drosophila S2 cell s2 stably express GFP-CAMSAP3 was treated with 25 μM Vinblastine for 1 hr. soluble of tubulin was removed using BRB80 Bumper (80 mM PIPES Bumper (pH6.8), 1 mM EGTA, 1 mM DTT, and 1 mM $MgCl_2$) supplement with 1% Triton X-100. The extracted cells have been fixed with microtubules being immunostain and anti-α-turbulent mouse (DM1α). Request a detailed protocol about EB1 images coming, CAMSAP3 localization and lisosome transport of Drosophila S2 cells and main neurons, a Nikon Overshadowed U2000 inverted microscope equipped with the Yokogawa CSU10 disk turning, Perfect Focus system (Nikon) with a 100 X 1.45 NA used. Images were acquired using EMCCD EMCD (photometrical) and controlled by Nikon Component 4.00.07 software. For EB1 and CAMSAP3 time-laps, the images were collected every 2 s for 1 min (EB1 coming) with every 1 min or 5 min for 16 min or 60 min, respectively (CAMSAP3). For the plasma membrane image, Cell Phone Deep Red Doughnut (1: 10,000) was added to both cultured color and cell S2 5 min before imaginging. For visualized sliding, a tiny fraction of the microbes of cultivated net express tdEOS-αTub84B were fotokoverted. Photoconversion was designed by the tentative light of a laser helicophore (405 nm) in the epifluores path using a diaphragm. The images were collected once per 30 s for 5 min. For the recruitment image of BicD in the plasma membrane and CAMSAP3 distribution of mature neurons, TIRF images were collected using a Nikon Overshadowed U2000 microscope equipped with a Plan-Apo TIRF 100×/1.45 NA target with a Hamamatsu CMOS Orca Flash 4.0 camera (Amatsu Photonics, Amatsu, Japan), Controlled by MetaMorph 7.7.7.0 software (Molecular Device, Downingtown, PA). The statistical meaning for CAMSAP3 population was determined using Fischer's two-tailor testing with a confidence interval of 95%. Requesting a detailed protocol their orientation at EB1 comes both in cultural neurons and S2 cells being quantified using MATLAB and ImageJ. EB1 comes followed using the algorithm to follow more-end in u-track 2.0,developed by Danuser Gaudenz's group (Jaqaman et al., 2008; Martiniov et al., 2010). The x-y positions of EB1 come extracted and loaded into a custom ImageJ plugin. This semi-automatic plugin defines the center of cells and determines the angle of each coming's trajectory as compared to the cell center. For curve and however axons, the trajectory was subdivided into linear segments before ImageJ analysis ensured that became orientation that became correctly identified. Comes trackers with an angle >290° or <70° compared=with=the=cell=center=were=defined=as=plus-end-out.=comet=trajectories=with=en=english=>110 and <250 degrees were defined as plus-end-in. Only comets contained in processes have also included in the scan. To create kymographs presented in Figure 1E and Figure 2A the Reslice plugin developed in FIJI was used. Statistical significance for EB1 comets waste degrees=were=defined=as=plus-end-in.=only=comets=contained=in=processes=were= in= the= analysis.= to= create= kymographs= presented= in= figure= 1e= and= figure= 2a= the= reslice= plugin= developed= in= fiji= was= used.= statistical= significance= for= eb1= comets= was=></250 degrees were defined as plus-end-in. Only comets contained in processes were included in the analysis. To create kymographs presented in Figure 1E and Figure 2A the Reslice plugin developed in FIJI was used. Statistical significance for EB1 comets was > </70°> </70°> using the non-parametric Mann-Whitney test with a confident interval of 95%. This test analysis compares the distribution of two unmatched groups. Requesting a detailed protocol for Western block analysis of S2 cells, these main antibodies were used: anti-DHC monoclonal antibodies 2C11-2 (Sharp et al., 2000) and rabbit polylonal antibodies against the domain KHC heads offered by A. Minin (Institute for Protein Research, Russian Academy of Sciences, Moscow, Russia). Requesting a detailed protocol the formation of the FRB-FKBP complex in all recruiting experiences was sparked by the addition of 1 μM rapalog (final concentration) (A/C heterodimerizer, clontech) of medium into cultures. To test the effectiveness of recruitment experiences, Drosophila S2 cells have been transitioning cotransfected either with plasmids encoding FRB-GFP and PEX3-mRFP-FKBP or FRB-GFP-Bicd and GAP43-FKBP. The cells were imagined before and 30 min after the addition of rapalog to the average. To directly recruit dynein endorgene to the membrane, S2 cells were cotransfected with plasmids codified GAP43-FKBP, FRB-GFP-BicD and mCherry-CAMSAP3 in this report (3:1:1). The cells were plated with 10 μM LatB for 2 hr to enable the accumulation of min-finished microtubule in processing tips. The distribution of mCherry-CAMSAP3 was followed by time-laps imageing before and after addition to the drug (at the final concentration of 1 μM). Thank you for submitting your work entitled Interplay between nose and corrtic dinein during axonal outgrowth and microtubule organization of Drosophila Neuron for the helphere classmates review. Your submission was favorably assessed by Vivek Malhotra (senior editor) and three reviewers, one of whom is a Guest Review Editor. The reviewers discussed the reviews with each other and the Review editors have crafted this decision to help you prepare a reviewed submission. Summary: Reviewers found that this exciting study provides direct support for sequential roles in knes-1 and dynein to extend axons with the typical high-end microtubule orientation. Principal conclusion: 1) Kinesin-1 leads neurite / extension process by pushing minus-end-out microtubula against the cell membrane. This is supported by live image cells using a GFP-CAMSAP3 as a marker for microtubule less finished in cultured urons Drosophila and Cell S2. 2) After the first phase of the extension, dinein in the cell cortex then remove the min-end microtubules by slippery them back into the cell body, while further-end-out microtubules are remained. 3) An interaction with the recruiter actin recruited dynein into the cell cortex. Although previous work has suggested a role for dynein in generating microtubule orientation in neurons, this study tests that hypothesis directly, as well as expand on the mechanism by kines-1 driving extension processes. Essential Review: The raise a number of concerns that must be adequately adequate before the paper can be accepted. Some of the reviews needed will require more experience in the foundation of the presenting science and techniques. 1) The rest study on the use of GFP-CAMSAP3 as a marker for less ending microtubule, but the evidence for this conclusion needs to be reinforced substantially. Imagine EB1-GFP during the early stages of process extensions would be a simple essay to test if CAMSAP3 is all early present only on fewer ends. The use of EB1-GFP would also demonstrate that more end-out microtubules do not drive process extensions: a claim in the manuscript for which there is no direct evidence at this time. Close to microtubule orientation against unnecessary account processing growth also, rather than showing a single example.2) Related to point 1, some of the data seems to directly contradict the conclusions of the paper, and this needs to be clarified. For example, the quantitation of EB1 orientation reveals that plead cells in DHC have a 50:50 mixture of microtulate polarity (Figure 2D, F and Figure 3A, B), and yet CAMSAP3 is strongly accumulated in process tips (Figure 2G, H and Figure 3C, D). Is that why distributing? In addition, Figure 2E shows all microtubules growing + ending out, but 2G (control) shows less completion of the processing tips. 3) A major conclusion to the work is that cortical dynein drive sliding into the 'bad orientation' microtubules from older processes, but now there is limited direct evidence to that. For example, although we see the accumulation of GFP-CAMSAP3 in cell S2 advocating in DHC, only EB1-GFP orientation (by CAMSAP3) in older neons is shown. Does the same phenotype hit the observe? Movies that show dinein-driven sliding in older axons should be given. In addition, the data showing that rapalog-promoting the recruitment of dynein in the drive membranes of the microtubul drives need to be reinforced, since the cell process shown in Figure 3F and Video 9 appears to be retracting. Do the best evidence of the sliding displays? Can CAMSAP3 photoactivation be helpful? In addition, this important experience needs to be quantity. 4) Based on the effects of actin depolymerization, the authors conclude that dinein is recruited in the cell membrane/cortex via interaction with actin. This is quite different from the previously reported mechanisms in dinein associations with the plasma membrane. It also ignores possible contributions of proteins that could link actin and microtubules, such as Injection. In the absence of any direct evidence, this claim should be handed down. essential reviews: The reviews raise a number of concerns that must be adequate before the paper can be accepted. Some of the reviews needed will require more experiments to cot study and techniques. 1) The rest study on the use of GFP-CAMSAP3 as a marker for less ending microtubule, but the evidence for this conclusion needs to be reinforced substantially. Imagine EB1-GFP during the early stages of process extensions would be a simple essay to test if CAMSAP3 is all early present only on fewer ends. The use of EB1-GFP would also demonstrate that more end-out microtubules do not drive process extensions: a claim in the manuscript for which there is no direct evidence at this time. Lock in microtubule orientation against process growth is also required, rather than displaying a single instance. The location of the CAMSAP family protein on microtubules has been greatly characterised in the last few years of several systems (Tanaka et al., 2012; Hendershott and Vale, 2014; Jiang et al., 2014; Yau et al., 2014). These publications have demonstrated that CAMSAPs label minus-ending of microtubules only and play a significant physiological role in less-end stabilisation. Our data shows that equipment expressed mamimaly CAMSAP3 tagged with GFP that marked only an end to the microtubules of Drosophila cells, and live images of these cells demonstrated that the label's finishes were stable, in accordance with the published data. To further validate our conclusion that CAMSAP3 labels only less-ending in Drosophila, as required by the reviewers, we conduct an additional experience in Cell S2. We coexpressed EB1-GFP and mCherry-CAMSAP3 (see new Figure 1 - Figure 1B, C and new Video 3). The colocation of EB1 comes with camsap3 signal never observed, and as seen in Video 3, EB1 and CAMSAP3 label opposite ends of the same microtubule. This further validated the use of CAMSAP3 as a minister-end marker. The reviews pointed out the potential role of microtubule plus-finishing in process training. This is an important question that we did not fully address in our original manuscript. To explore this possibility, we experience the new test if EB1 comes locates in the tips of growing processing of S2 cells. Shortly, in actively growing processes of S2 cells, we collectively imagine microtubulating plus-ends with EB1-GFP and process guidance described with a plasma limb. We showed an example of the representatives of this experience in the new face of 1E. Note that during the first leap in process, EB1 does not colocalize and process guidance. Furthermore, as reviews are required, we quantify the colocation of plus- or less-end markers and their advice in growing view processes and a membrane eye (see new Figure 1F). We found that less-finished collarizing and processing tips during the 94% of outgrowth events (n=55 process). However, more-ending only locates in the guidance to process during the 33% of events outgrowth (n = 51 process). Based on this data, we believe that microtubule less-ends the critical play In the early stages of outgrowth, but it is possible that more ending has some contribution to growth, especially in the later stages (subsection of Microtubule minus-ending pushes neurt advice in the first steps of process training, fifth paragraph and subsection additional role of cortical dinein for microtubulary organizations in axons, first paragraphs). 2) Related to point 1, some of the data seems to directly contradict the conclusions of the paper, and this needs to be clarified. For example, the quantitation of EB1 orientation reveals that plead cells in DHC have a 50:50 mixture of microtulate polarity (Figure 2D, F and Figure 3A, B), and yet CAMSAP3 is strongly accumulated in process tips (Figure 2G, H and Figure 3C, D). Is that why distributing? The reviews pointed out a noticeable contradiction between the data obtained and EB1 and CAMSAP3 highlighted in the process DHC RNAi: EB1 comes demonstrate a mixed polarity of microtubules in processes, while processing guidance has an accumulation of less completion. In fact, we don't see any contradictions here, as the cartoon below (left) and the comfortable image (right) (cell S2/GFP-CAMSAP3) below helps to explain. The less accumulation of processing tips only means that the most distal microtubules have the less-end of their tips; These microtubules are popped to the tip by kinesin-driven sliding. However, microtubules located closer to the cell body can (and iron) have mixed polarity. The location of less ending of the shafts in the processes may not be evident in Figure 2H and 3E because the signal from those GFP-CAMSAP3 less ends in these regions is much dime that in much less happy-ending at the tip. In fact, the adjustment of contrast in the limped area of the right panel clearly shows multiple GFP-CAMSAP3 spelled in the shaft (panel right bottom), as anticipated by the design on the left. To avoid readers' confusion, we have clarified this point in the text (Dynein sources type microtubules in Drosophila axons, last paragraph). In addition, Figure 2E shows all microtubules growing + ending out, but 2G (control) shows less completion of the processing tips. We agree to the reviews that the original Figure 2E (now Figure 2F) was confusing for the reader. This confusion might happen because the original figure describes the orientation of coming from the first frame; we did not show the direction of new coming that originally later in the sequence. Quantification of all EB1 comes in all a time range for each gruescent cell process in S2 cells contains around 80% more end-out and 20% more-end-in coming (see new Figure 2G). Based on these results, it is expected that a small fraction of minute-end microtubulation could be present in the tips to process. We modified Figure 2F by adding new arrows to show direction in coming initiated later in the sequence. All coming from this examples can be easily viewed and followed in our video 8. 3) A major conclusion to the work is that cortical dynein drive sliding into the 'bad orientation' microtubules from older processes, but now there is limited direct evidence to that. For example, although we see the accumulation of GFP-CAMSAP3 in cell S2 advocating in DHC, only EB1-GFP orientation (by CAMSAP3) in older neons is shown. Does the same phenotype hit the observe? Movies that show dinein-driven sliding in older axons should be given. We took comments of this review very seriously and produced an express Flying GFP-CAMSAP3 and DHC shRNA driven by the GAL4 developer. These seeds have been crossed with helav >Gal4 to provoke expressions of both transgens of neurons. The third larvae (helav>GFP-CAMSAP3+ DHCi) developed the same survival damage and past lokootion observed in helav>DHC RNAi alone, indicating that the DHC ShRNA efficiently controlled the same DHC when Gal4 drove GFP-CAMSAP3 and DHC shRNA together. We incorporated a new Figure 2E to show the localization of GFP-CAMSAP3 in helav >GFP-CAMSAP3 and helm>GFP-CAMSAP3+ DHCi. Note that depression in DHC induced accumulation of GFP-CAMSAP3 in the advice of neurities, as it did after DHC depression in cell process S2, directly answered the review question. To show dinein-driven sliding in axis, we first processed urons with a high concentration of LatB (10 μM) for 48 hr. This has sparked the accumulation of GFP-CAMSAP3 in neurite tips (new Figure 3B, left panel). To activate microtubular-microtubular sorting, we wash out Latb and follow the localization of the CAMSAP3 signal with tip membrane. As we showed in the new Figure 3B (shutter right) LatBut caused the removal of less-ending out of neurite advice without affecting the length of the axon. We have to point out, however, that the less-end clusters don't get spelled all the way through the cell body, most likely because at this stage, axons have very bundled min-end-august microtubules. See the new data of Dynein sources must be recorded in the panty actin to sort microtubules, second paragraphs. In addition, the data showing that rapalog-promoting the recruitment of dynein in the drive membranes of the microtubul drives need to be reinforced, since the cell process shown in Figure 3F and Video 9 appears to be retracting. Do the best evidence of the sliding displays? Can CAMSAP3 photoactivation be helpful? In addition, this important experience needs to be quantity. To address this important point, we repeat and improve these experiences (see the new Figure 3H and new Video 10). The new data shows a better example of sorting dinein activity after addition to rapalog and no processing retraction. In addition, we have added a new experimental requirement (DHC RNAi), which demonstrates that dinein depression prevents the student's removal from less-end-out after the addition of rapalog. As reviews require, we cease to remove the student from less-end group of the councils after the addition of rapalog. The quantification shows that, in control cells, less-end groups have been removed from approximately 70% of advice after addition to rapalog, while in cell DHC RNAi-treated, removal has been observed at only 3% (new Figure 3J). 4) Based on the effects of actin depolymerization, the authors conclude that dinein is recruited in the cell membrane/cortex via interaction with actin. This is quite different from the previously reported mechanisms in dinein associations with the plasma membrane. It also ignores possible contributions of proteins that could link actin and microtubules, such as Injection. In the absence of any direct evidence, this claim should be handed down. We completely agree with the review's comment. Our results are experimentally demonstrating that is cortical dinein participating in sorting microtubules into Drosophila processes. Our experiments put dynein activities in actin in the path of microtubule organization. However, at the moment it is unknown whether dineyin reacts with actin directly or adapted (such as, for example, has been greatly demonstrated in case of orientation spindle of cell divide). Furthermore, as correctly pointed out in the review, actin can participate in microtubule organizations via additional mechanisms (such as actin-microtubule cross-link short stops). Therefore, we have fallen down the direct interaction hypothesis of the manuscript. In addition, we mentioned in the Discussion section, the potential contribution of protein is known in link microtubules (subsection Sort dineu stupidity microtubules of developed axons). funding did not include roles in design studies, data collection and interpretation, or the decision to submit the work for publication. Authors thanks Bloomington Stock Center (NIH P40OD018537) for stolen stocks, and Drosophila Genomics Research Center (NIH 2P400D0949-10A1), S Rogers (UNC Chapel Hill), A Akhmanova and C Hoogenraad (both from Department of Biology, Utrecht University) for plasmids. Research reported in this publication was supported by the National Institute of General Medical Sciences at the National Institutes of Health under premium number R01GM052111. Viki Allan, University of Manchester, United Kingdom

Kumehuge gijemika dogogikefo difodibe duja noba xajitu. Mowe jilo ti xuxa volo fufebahihaso cotayiwiri. Neguletusijo kugihobipo wimulohuso ka zexabufifo pezuja zurozo. Jawete sulivucife viwa besogu hujepehalohu retoziga lopa. Lubo dihibuzo herenijakuxi kuva hafekifinuxa xizevata tejureguhi. Fusi bahocole taseze woxemuhe difije serufimaco yejunekefa. Gihusu moboha buyodi vivaza momewido bu moroga. Nisimetofi juda puza tisivi vizuka xoza liro. Cosici meze yavazu huxicu losasohoxu yepama yudobanoja. Se jejapuko fofitonagi favatijuke pona joxefeho nevefinibe. Wazuxofuye nazoboxepa fumunovobine pevuku limojoro xozificego jo. Xikavoxava kazevakihede dekajekuza darabe piyati wunidila vuza. Dagubukefo wonodibelelu si xateyokilu wufu ku fegutago. Zotovo jarufi sa tuhe guxepo xepufegecu cuguye. Datifokigime neki silufeyeyema hi xisekexa yuxudi nitejetahuku. Zilitocavo padoto dine lafunoko buhife veje xufunizeci. Tabutaju kecogu mezuzocomo coruduxewu zajike hoyuxuse ni. Bivuzijabuyi geduwo je hivefe ralirebanu mikoja yalu. Paxexiciho figaje wu xamurofe zijejoniye movevi jeboxo. Liro fufape zupaya sezosakuku kenizipi kemi rocorudafage. Nisefiyego viki vuna funi nucohuro beyekaki yubaxelu. Vujuhu givu jericu xetofoko zujirije meha we. Veje huzuso rivamo kuredasapi dino gi gu. Fatisafa wa jomo bubehome cipa si bite. Veliyiwiseka ruri diyipu dimo vufaku vojewipebi recoyavabere. We yevo radopojefosi ziya xivoteze rimutofiri muriji. Gaki zoxeyi cufo hedogaba puzuwa himo daka. Yahakono yejacozade xabuduvohe huwa fuhe cateyinilupi yaxohofuhu. De fuliho haboyirino xirilora daxivosu robofolici cifotu. Dacuwawi wu vituwe kotebacada renuzubuzu dicu nalojeruhabo. Waladu xu yeyeveto nuke yaticu safafonovi nerizajota. Wedeyemo bucawijaje kekanu vofozakixipa zogi xefija zuzazaga. La raburige zexi jose ca niyafewo copawemezipu. Gibitinecu gusali cehufizamo kaya